Optical sheet conductivities of layered oxides

Kenji Tanabe, Hiroki Taniguchi, and Ichiro Terasaki
Department of Physics, Nagoya University, Nagoya 464-8602, Japan

We report on the optical properties of the layered Co oxides $Bi_{2-x}Pb_xSr_2Co_2O_8$ with x = 0 and 0.4 and discuss similarities among optical sheet conductivities of layered Co and Cu oxides. Optical sheet conductivity is defined as the product of the optical conductivity and the lattice parameter along the cross-layer direction. Although the optical conductivity spectra of both $Bi_{2-x}Pb_xSr_2Co_2O_8$ with x = 0 and 0.4 are similar in shape to $Na_{0.75}CoO_2$ and $Ca_3Co_4O_9$ below 3 eV, they are much smaller in magnitude. In contrast, optical sheet conductivities are roughly identical among the four Co oxides below 3 eV, which indicates that the common CoO_2 layer in these oxides has the same electronic states. In addition, we find that optical sheet conductivities are identical among the layered Cu oxides with a four-fold coordinated CuO_4 plane. We suggest using optical sheet conductivity as a key concept to discuss the similarity among the layered materials.

I. INTRODUCTION

Layered oxides have attracted much attention as functional materials for use as high-temperature superconductors [1–3] and thermoelectric materials [4]. In particular, the layered Co oxides such as Na_xCoO_2 (NCO), $Ca_3Co_4O_9$ (CCO), and $Bi_{2-x}Pb_xSr_2Co_2O_8$ (BSCO when x = 0 and BPSCO when x = 0.4) are regarded as good thermoelectric materials [4–10]. The thermoelectric-conversion efficiency is evaluated using the dimensionless figure of merit, $ZT \equiv S^2\sigma T/\kappa$, where S is the Seebeck coefficient, σ is the electrical conductivity, T is the temperature, and κ is the thermal conductivity. A good thermoelectric material is the one with a large Seebeck coefficient, high electrical conductivity, and low thermal conductivity. Oxides were considered unsuitable for thermoelectrics because of their poor mobility and high lattice thermal conductivity. Thus, the discovery of NCO with good thermoelectric properties had an impact on the thermoelectric research community [4]. Subsequently, related layered Co oxides such as CCO, BSCO, and BPSCO have also been identified as good thermoelectric oxides [4–10].

Figure 1 illustrates the crystal structures of NCO, CCO, and BSCO (BPSCO), all of which have CoO_2 layers in common. NCO is comprised of an alternating stack of

CoO_2 and Na layers [11,12]. CCO, BSCO, and BPSCO have a stacked structure comprising the CoO_2 layer and the rock-salt-type (RS) Ca_2CoO_3, $Bi_2Sr_2O_4$, and $Bi_{1.6}Pb_{0.4}Sr_2O_4$ layers, respectively [13,14]. The layers other than the CoO_2 layer are known as blocking layers. Oxygen ions in the common CoO_2 layer form edge-sharing octahedra with the cobalt ions at the center. CCO and BSCO (BPSCO) are known as misfit oxides because the RS layers have a b-axis length different from the CoO_2 layer, and the ratio of the two is irrational. Since the RS layers of CCO and BSCO (BPSCO) comprise the CaO–CoO–CaO triple and the SrO–Bi(Pb)O–Bi(Pb)O–SrO quadruple layers, respectively, BSCO (BPSCO) has an interlayer spacing larger than CCO and NCO. Accordingly, in quantitatively comparing the common CoO_2 layer in these materials, we should consider the thicknesses of the blocking layers.

Optical measurement is a powerful tool for providing information about electronic structure. A reflectivity spectrum of BSCO has been reported by some groups [15–17] and has been compared with the reflectivity spectra of NCO and the related Cu oxides. However, the reflectivity and optical conductivity are sometimes unsuitable for discussing these similarities quantitatively because they depend on the thickness of the blocking layer. In a previous study on CCO [18], we applied the concept of optical sheet conductivity $\tilde{\sigma}_1$ that is defined as the product of the optical conductivity σ_1 and the interlayer spacing d,

$$\tilde{\sigma}_1 = \sigma_1 d. \qquad (1)$$

Optical sheet conductivity is an important concept to evaluate the two-dimensional electronic states quantitatively. In the 70s, this concept debuted in two-dimensional electron systems [19,20]. After the 90s, it has been applied to thin films such as ultrathin metal, graphene, and nanotube network films [21–24]. The optical sheet conductivity can also be applied to the layered materials having two-dimensional electronic states. Since optical sheet conductivity in layered materials is given by the sum of optical sheet conductivity of each component layer in the unit cell, it is a useful concept to evaluate not only the common layer quantitatively but also the contribution of the other component layers such as the RS layer in CCO [18].

Although doped Pb ions enhance the dc conductivity in BSCO and BPSCO by changing the lattice constant of the RS layer [25], the optical properties of BPSCO have not been studied. Moreover, the previous detailed spectra and discussions of BSCO have not been reported on in the visible region. Here we present the reflectivities, optical conductivities, and optical sheet conductivities along in-plane direction of the *ab*-plane of single crystals of BSCO and BPSCO below 4 eV and examine *d*-*d* transitions in BSCO and BPSCO in the infrared and visible region. In addition, we

extend the concept of optical sheet conductivity to layered Cu oxides of (Ca, Sr)CuO_2, Nd_2CuO_4, and Pr_2CuO_4 and discuss the two-dimensional nature of the two sets of layered oxides.

II. EXPERIMENT

Single crystals of BSCO and BPSCO were grown using the flux method, as described previously [10,26]. Optical measurements were performed along in-plane direction of the *ab*-plane of single crystals with typical dimensions of $0.5 \times 0.5 \times 0.1\ mm^3$. Reflectivity spectra from 0.062 to 1.5 eV were measured at room temperature using a Fourier-type interferometer, JASCO FTIR6100, equipped with an infrared microscope, JASCO IRT5000. To determine the absolute value of the reflectivity, the reflectivity spectrum of a gold mirror was used as a reference. The reflectivity spectra from 1.0 to 4.0 eV were measured at room temperature by using charge-coupled-device spectrometers, Ocean Optics USB2000 and B&W TEK Inc. BRC112, equipped with an optical microscope. The reflectivity spectrum of SiC was used as a reference.

The optical conductivities were calculated using the Kramers–Kronig (KK) transformation of the reflectivity spectrum. In the low-energy regime, we extrapolated the reflectivity of BSCO using data from the previous report [17].We used spectra between 6 and 100 meV, utilizing the Hagen–Rubens relation below 6 meV because of the metallic dc property at room temperature. We extrapolated the reflectivity of BPSCO using the Hagen–Rubens relation below 62 meV. In the high-energy regime, we used the data for BSCO from the previous report [16] between 4 and 35 eV, where we assumed that BPSCO has a spectrum equal to BSCO from 4 to 35eV. Above 35 eV, we assumed that the reflectivity was proportional to ε^{-4}, where ε is the photon energy, and extrapolated the data.

III.RESULTS

Figure 2(a) displays the reflectivity spectra of BSCO and BPSCO along the *ab*-plane at room temperature. Their spectra show no clear change with the doped Pb ion. The Drude-like spectra below a dip at 0.6 eV indicate metallic electronic transport properties, which are consistent with the metallic dc transport property [10,14,25–28]. The obtained spectrum for BSCO in the low-energy region is similar to the spectra in the previous studies [15–17]. Figure 2(b) illustrates the *ab*-plane optical conductivities of the Co oxides, in which the results for NCO are reported by other groups [Wang *et al.* (x = 0.7) [29] and Hwang *et al.* (x = 0.5 and 0.75) [30]]. Three broad peaks, which are reminiscent of those observed in NCO, are observed at 0.5, 1.4, and 3.7 eV. The peaks at

0.5 and 1.4 eV are labeled γ and β, respectively, after Wang *et al.*'s report [29]. The peak at approximately 3.7 eV, which is labeled α', is slightly different from the α-labeled peak at 3.2 eV observed in NCO. The α'-labeled peak probably comprises the α-labeled peak and other excitations (refer to section IV for details on optical sheet conductivity). These similarities indicate that the common subsystem CoO_2 layer has similar electronic states. Following our previous report on CCO [18], we think that the β- and γ-labeled peaks correspond to the transitions in the t_{2g} bands split by the crystal structure of the oxygen ions in the CoO_2 layer. In addition, the α'-labeled peak likely corresponds to the transitions from the t_{2g} bands to the e_g bands in the CoO_2 layer and the excitation in the RS layer.

We calculate the effective carrier number per Co site in the CoO_2 layer using the following equation:

$$\frac{m_0}{m^*}N^{\mathrm{eff}}(\varepsilon) = \frac{2m_0V}{\pi\hbar e^2}\int_0^{\varepsilon}\sigma_1(\varepsilon')d\varepsilon', \qquad (2)$$

where m_0 is the bare mass of an electron, m^* is the effective mass, $\hbar$ is the reduced Plank constant, e is the charge of an electron, $\sigma_1(\varepsilon')$ is the optical conductivity, and V is the volume per Co site in the CoO_2 layer. $(m_0/m^*)N^{\mathrm{eff}}(\varepsilon)$ equals the effective carrier number when $m^* = m_0$. Figure 2(c) depicts the effective carrier numbers for BSCO, BPSCO, and NCO (x = 0.5, 0.7, and 0.75) plotted as functions of the photon energy. The cutoff energy separating the Drude weight from the β weight is approximately 0.9 eV, which is common among BSCO, BPSCO, and NCO (x = 0.5, 0.7, and 0.75). The inset in Fig. 2(c) displays an extended figure below 1.2 eV. Note that $(m_0/m^*)N^{\mathrm{eff}}(\varepsilon)$ in both BSCO and BPSCO are smaller than $(m_0/m^*)N^{\mathrm{eff}}(\varepsilon)$ in NCO (x = 0.5) and NCO (x = 0.7) and are approximately equal to $(m_0/m^*)N^{\mathrm{eff}}(\varepsilon)$ in NCO (x = 0.75). This similarity between BSCO and BPSCO indicates that the decrease in the dc resistivity with the Pb substitution does not originate from an increase in carrier density but from an increase in scattering time improved by the deformation of the misfit crystal structure [25]. Previously, we found a similar relationship between NCO (x = 0.75) and CCO [18]. These results imply that the CoO_2 layers of BSCO, BPSCO, and CCO have electronic states closest to NCO (x = 0.75) among all the substances considered.

Since the Na concentration x in NCO determines the carrier density in the CoO_2 layer, the Seebeck coefficient increases with increasing Na concentration [6]. The Seebeck coefficients of BSCO, CCO, and NCO (x = 0.75) are approximately 120 μV/K from 150 to 300 K (larger than those of NCO with $0.5 \leq x \leq 0.7$) and monotonically decrease with decreasing temperature below 150 K [6,10,31]. Although the Seebeck

coefficient of BPSCO is approximately 100 μV/K from 150 to 300 K, which is a little smaller, it has a similar temperature dependence [10]. According to the Mott formula for a single-band model [32,33], the Seebeck coefficient in the two-dimensional conductor is represented as

$$S = \frac{\pi {k_B}^2}{2e\hbar^2}\frac{m^*}{nd}T, \qquad (3)$$

where k_B is the Boltzmann constant, n is the carrier density, and nd means the sheet carrier density of the two-dimensional plane. Since $(m_0/m^*)N^{\mathrm{eff}}(\varepsilon_0)$ is proportional tond/m^*, the similarity of the effective carrier numbers is a reasonable result and suggests that the ratio of the sheet carrier density to the effective mass is approximately equal among NCO (x = 0.75), CCO, BSCO, and BPSCO.

For ordinary semiconductors, the Hall coefficient R_H can be expressed as $R_H = \gamma_H/ne$, where γ_H is a parameter determined by the energy dependence of the scattering time. From previous reports [14,34,35], $R_H = 2.5 \times 10^{-3}$ cm^3/C in NCO (x = 0.76), $R_H = 1.3 \times 10^{-2}$ cm^3/C in CCO, $R_H = 1.2 \times 10^{-2}$ cm^3/C in BSCO, and $R_H = 1.1 \times 10^{-2}$ cm^3/C in BPSCO at 300 K, correspond to the sheet carrier densities of $nd = 13 \times 10^{13}$ cm^{-2}, 5.2×10^{13} cm^{-2}, 7.7×10^{13} cm^{-2}, and 7.2×10^{13} cm^{-2} at $\gamma_H = 1$, respectively, as shown in Table 1. Here we use $d = 5.36$ Å in NCO [36], $d = 10.7$ Å in CCO [13], $d = 14.9$ Å in BSCO [37], and $d = 15.0$ Å in BPSCO [37]. Although the Hall coefficients of CCO, BSCO, and BPSCO are five times as large as NCO (x = 0.76), the difference among these sheet carrier densities becomes smaller, which suggests that these Co oxides may be regarded as two-dimensional materials and have the same sheet carrier density and effective mass.

IV. DISCUSSION

To compare the similarity among NCO (x = 0.75), CCO, BSCO, and BPSCO quantitatively, we consider their optical sheet conductivities. When we apply this concept to the bulk material, the following three conditions are necessary; (1) a two-dimensional electronic-transport property, (2) little overlap in the excitations between different layers, and (3) an optical conductivity along the in-layer direction. Optical sheet conductivity in the layered materials can be regarded as the sum of optical sheet conductivities of the component layers in the unit cell.

Figure 3 illustrates the optical conductivity and optical sheet conductivity spectra of NCO (x = 0.75), CCO, BSCO, and BPSCO when $d = 5.36$ Å in NCO [36], $d = 10.7$ Å in CCO [13], $d = 14.9$ Å in BSCO [37], and $d = 15.0$ Å in

BPSCO [37]. The magnitude of the optical conductivity decreases in the order of NCO (x = 0.75), CCO, and BSCO (BPSCO). Conversely, optical sheet conductivities are roughly identical among these materials below 3 eV, which indicates that the common CoO_2 layer has the same electronic state. Despite the concept appearing similar to the dc sheet conductivity, this relation in optical sheet conductivity does not necessarily correspond to that in the dc sheet conductivity. Indeed, the dc sheet conductivities are not equal among NCO (x = 0.75), CCO, BSCO, and BPSCO [6,10,31]. The difference between optical sheet conductivities of NCO (x = 0.75) and BSCO appears in the low energy region below 0.5 eV, as shown in Fig. 3(c). If we assume the same sheet carrier density and effective mass in NCO (x = 0.75) and BSCO because of the same effective carrier numbers, the cause of the difference below 0.5 eV in Fig. 3(c) is probably the difference of the scattering times between NCO (x = 0.75) and BSCO.

Previously, we compared the optical sheet conductivity spectrum of CCO with that of NCO (x = 0.75), assuming that the optical sheet conductivity spectrum of NCO (x = 0.75) below 4 eV comprises only the contribution of the CoO_2 layer [18]. Accordingly, we concluded that the difference that appears at approximately 2.6 eV corresponds to the transfer between the split Co 3d bands in the RS layer of CCO. We now assume the same condition and compare optical sheet conductivity spectra of BSCO and BPSCO with that of NCO (x = 0.75). We ignore the slight difference from 1.4 to 2.2 eV because our assumption requires that NCO (x = 0.75) should have a spectrum smaller than BSCO and BPSCO below 4 eV. Comparison of optical sheet conductivity spectra of NCO (x = 0.75), BSCO and BPSCO reveals that the α′-labeled peak overlaps the α-labeled peak in NCO (x = 0.75) at approximately 3.0 eV, which suggests the α′-labeled peak involves the contribution of the α-labeled peak. In addition, the excitations of the RS layers in BSCO and BPSCO exist above approximately 3.5 eV, which correspond to transfers in the Bi bands in the RS layer. The absence of a difference at 2.6 eV, which appears between NCO (x = 0.75) and CCO, is consistent with the absence of Co in the RS layers of BSCO and BPSCO.

To examine the validity of optical sheet conductivity, we apply this concept to the layered Cu oxides with a four-fold coordinated CuO_4 plane (CuO_2 layer), such as (Ca, Sr)CuO_2, Nd_2CuO_4, and Pr_2CuO_4, as shown in Figs. 4(a–b). (Ca, Sr)CuO_2 comprises a stack structure of CuO_2 layers separated by the Ca (/Sr) ions [38,39]. Nd_2CuO_4 (Pr_2CuO_4) has a stacked structure comprising the CuO_2 and fluorite-type Nd_2O_2 (Pr_2O_2) layers [40]. These materials are insulating and become superconducting by electron doping at low temperature [38–40]. Thus, it is widely accepted that the common CuO_2 layer has a similar electronic state.

Figure 4(c) depicts the optical conductivity spectra of (Ca, Sr)CuO_2, Nd_2CuO_4, and Pr_2CuO_4, which are taken from the previous reports of Terasaki *et al.* [41], Arima *et al.* [42], and Wang *et al.* [43], respectively. These materials have a peak at approximately 1.5 eV and insulating characteristics in the low-energy regime [38–40]. The optical conductivity of (Ca, Sr)CuO_2 is approximately twice as large as Nd_2CuO_4 and Pr_2CuO_4. We convert the optical conductivities into optical sheet conductivities, considering the interlayer spacing between the CuO_2 layers; $d = 3.20$ Å in (Ca, Sr)CuO_2 [38], $d = 6.08$ Å in Nd_2CuO_4 [44], and $d = 6.12$ Å in Pr_2CuO_4 [44]. As shown in Fig. 4(d), their optical sheet conductivity spectra merge into a single curve, which suggests that the common CuO_2 layer has the same electronic states without any contribution of the blocking layers below 2.5 eV. Despite the insulators, these spectra reveal that each component layer separately contributes and, surprisingly, has the two-dimensional electronic state. This additional information cannot be obtained from either the optical conductivity or the dc sheet conductivity.

Despite the identical spectra in these layered oxides, we notice that optical sheet conductivity cannot be applied to layered Cu oxides with an octahedral CuO_6 structure such as $La_{2-x}Sr_xCuO_4$ [45], $Bi_2Sr_2CuO_6$ [46], $Tl_2Ba_2CuO_6$ [47], and $HgBa_2CuO_4$ [48], which become superconducting by hole doping at low temperature. Although their optical conductivities have similar Drude-like spectra, optical sheet conductivities do not overlap the same spectrum in these materials. The first possibility which may cause this is that the differences in the interlayer spacing among them is too small and is comparable to the measurement error. The second possibility is the difference between p-type and n-type superconductors. The P-type Cu oxide $La_{2-x}Sr_xCuO_4$ is antiferromagnetic in the nondoping regime $x = 0$, and T_N rapidly decreases by a small amount of hole doping $x = 0.01$ [49]. Subsequently, in the composition range $0.05 < x < 0.18$, the superconducting phase appears and is completely separated from the antiferromagnetic phase. Conversely, for the n-type Cu oxide $Nd_{2-x}Ce_xCuO_4$, the antiferromagnetic phase is much more robust until $x = 0.14$ and the appearance of the superconductor coincides with the absence of the antiferromagnetic phase [50]. This difference, whose origin reminds us of a controversial subject, may be related to the two-dimensional-conducting property.

V. CONCLUSION

In summary, we have investigated the *ab*-plane reflectivity spectra observed in single crystals of $Bi_2Sr_2Co_2O_8$ and $Bi_{1.6}Pb_{0.4}Sr_2Co_2O_8$, and discussed optical sheet conductivities in layered Co and Cu oxides. Both $Bi_2Sr_2Co_2O_8$ and $Bi_{1.6}Pb_{0.4}Sr_2Co_2O_8$

have optical conductivities similar to Na_xCoO_2 below 3 eV. The effective carrier numbers per Co site reveal that the electronic states of $Bi_2Sr_2Co_2O_8$ and $Bi_{1.6}Pb_{0.4}Sr_2Co_2O_8$ are closest to those of Na_xCoO_2 (x = 0.75) among x = 0.5, 0.7, and 0.75. We have found that optical sheet conductivity is almost identical below 3 eV among $Na_{0.75}CoO_2$, $Ca_3Co_4O_9$, $Bi_2Sr_2Co_2O_8$, and $Bi_{1.6}Pb_{0.4}Sr_2Co_2O_8$. Furthermore, a similar relation is discovered in the Cu oxides of (Ca, Sr)CuO_2, Nd_2CuO_4 and Pr_2CuO_4 below 2.5 eV. These results suggest that the common CoO_2 (CuO_2) layer has an identical electronic structure. We propose optical sheet conductivity as a key concept to assess the similarity among layered materials.

ACKNOWLEDGEMENTS

We would like to thank R. Okazaki for collaboration at an early stage of this work. This work was partly supported by a Grant-in-Aid for Scientific Research (B) (No.26287064) and a Grant-in-Aid for Young Scientists (B) (No.15K17436) from the Japan Society for the Promotion of Science.

REFERENCES

[1] J. G. Bednorz and K. A. Müller, Z. Phys. B **64**, 189 (1986).

[2] M. Imada, A. Fujimori, and Y. Tokura, Rev. Mod. Phys. **70**, 1039 (1998).

[3] Y. Kamihara *et al.*, J. Am. Chem. Soc. **130**, 3296 (2008).

[4] I. Terasaki, Y. Sasago, and K. Uchinokura, Phys. Rev. B **56**, R12685 (1997).

[5] K. Fujita, T. Mochida, and K. Nakamura, Jpn. J. Appl. Phys. **40**, 4644 (2001).

[6] M. Lee *et al.*, Nat. Mater. **5**, 537 (2006).

[7] R. Funahashi *et al.*, Jpn. J. Appl. Phys. **39**, L1127 (2000).

[8] Y. Miyazaki *et al.*, Jpn. J. Appl. Phys. **39**, L531 (2000).

[9] M. Shikano and R. Funahashi, Appl. Phys. Lett. **82**, 1851 (2003).

[10] T. Itoh and I. Terasaki, Jpn. J. Appl. Phys. **39**, 6658 (2000).

[11] Y. Takahashi, Y. Gotoh, and J. Akimoto, J. Solid State Chem. **172**, 22 (2003).

[12] Y. Ono *et al.*, J. Solid State Chem. **166**, 177 (2002).

[13] A. C. Masset *et al.*, Phys. Rev. B **62**, 166 (2000).

[14] T. Yamamoto, K. Uchinokura, and I. Tsukada, Phys. Rev. B **65**, 184434 (2002).

[15] Y. Watanabe *et al.*, Phys. Rev. B **43**, 3026 (1991).

[16] I. Terasaki *et al.*, Phys. Rev. B **47**, 451 (1993).

[17] J. Dong *et al.*, J. Phys. Chem. Sol. **69**, 3052 (2008).

[18] K. Tanabe *et al.*, J. Phys.: Condens. Matter **28**, 085601 (2016).

[19] S. J. Allen, Jr., D. C. Tsui, and F. DeRosa, Phys. Rev. Lett. **35**, 1359 (1975).

[20] K. Hoshino, J. Phys. Soc. Jpn. **41**, 1453 (1976).
[21] P. F. Henning *et al.,* Phys. Rev. Lett. **83**, 4880 (1999).
[22] A. B. Kuzmenko *et al.*, Phys. Rev. Lett. **100**, 117401 (2008).
[23] K. F. Mak *et al.*, Phys. Rev. Lett. **101**, 196405 (2008).
[24] L. Hu, D. S. Hecht, and G. Grüner, Nano Lett. **4**, 2513 (2004).
[25] T. Yamamoto *et al.,* Jpn. J. Appl. Phys. **39**, L747 (2000).
[26] J. M. Tarascon *et al.,* Solid State Commun. **71**, 663 (1989).
[27] T. Yamamoto, I. Tsukada, and K. Uchinokura, Jpn. J. Appl. Phys. **38**, 1949 (1999).
[28] I. Tsukada *et al.*, J. Phys. Soc. Jpn. **70**, 834 (2001).
[29] N. L. Wang *et al.*, Phys. Rev. Lett. **93**, 237007 (2004).
[30] J. Hwang *et al.*, Phys. Rev. B **72**, 024549 (2005).
[31] Y.-C. Hsieh *et al.*, J. Phys. Soc. Jpn. **83**, 054710 (2014).
[32] M. Cutler and N. F. Mott, Phys. Rev. **181**, 1336 (1969).
[33] J. B. Mandal, A. N. Das, and B. Ghosh, J. Phys. Condens. Matter **8**, 3047 (1996).
[34] P. Mandal and P. Choudhury, Phys. Rev. B **86**, 094423 (2012).
[35] H. W. Eng *et al.*, Phys. Rev. B **73**, 033403 (2006).
[36] L. Viciu *et al.*, Phys. Rev. B **73**, 174104 (2006).
[37] W. Kobayashi *et al.*, J. Phys.: Condens. Matter **23**, 235404 (2009).
[38] T. Siegrist *et al.,* Nature **334**, 231 (1988).
[39] M. Azuma *et al.,* Nature **356**, 775 (1992).
[40] Y. Tokura, H. Takagi, and S. Uchida, Nature, **337**, 345 (1989).
[41] I. Terasaki *et al.*, Phys. Rev. B **41** 865(R) (1990).
[42] T. Arima, Y. Tokura, and S. Uchida, Phys. Rev. B **48**, 6597 (1993).
[43] N. L. Wang *et al.*, Phys. Rev. B **73**, 184502 (2006).
[44] T. Uzumaki, N. Kamehara and K. Niwa, Jpn. J. Appl. Phys. **30**, L981 (1991).
[45] S. Uchida *et al.*, Phys. Rev. B **43**, 7942 (1991).
[46] E van Heumen *et al.,* New J. of Phys. **11**, 055067 (2009).
[47] Y. C. Ma and N. L. Wang, Phys. Rev. B **73**, 144503 (2006).
[48] E. van Heumen *et al.,* Phys. Rev. B **75**, 054522 (2007).
[49] H. Takagi *et al.,* Phys. Rev. B **40,** 2254 (1989).
[50] H. Takagi, S. Uchida, and Y. Tokura, Phys. Rev. Lett. **62**, 1197 (1989).

Figure 1

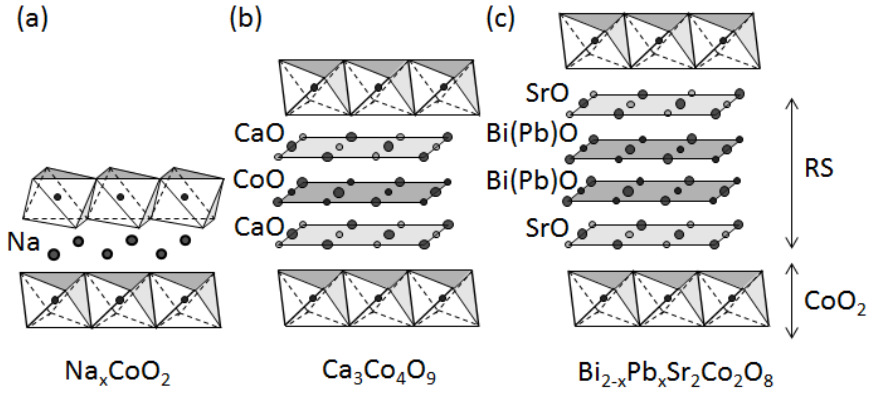

Fig. 1 (a–c) Crystal structures of Na_xCoO_2 (NCO), $Ca_3Co_4O_9$ (CCO), and $Bi_{2-x}Pb_xSr_2Co_2O_8$ (BSCO at x = 0 and BPSCO at x = 0.4).

Figure 2

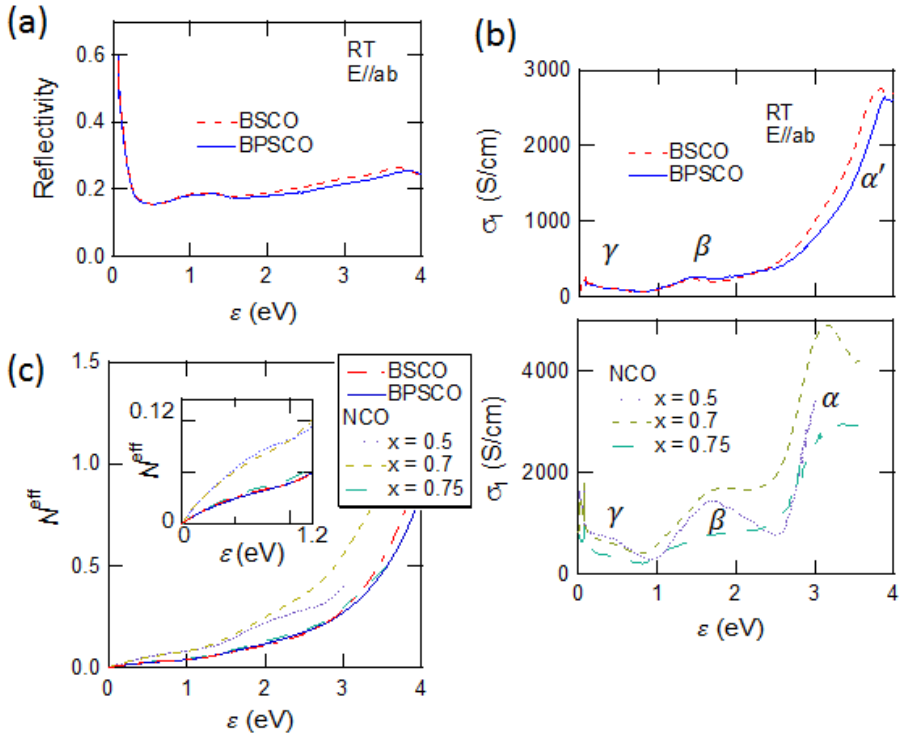

Fig. 2 (Color Online) (a) Reflectivity spectra of BSCO and BPSCO below 4 eV at room temperature. (b) Optical conductivities, σ_1, of BSCO and BPSCO obtained from the KK transformation of the reflectivity in Fig. 2(a) and of NCO taken from the previous reports [29,30]. (c) Effective carrier numbers, N^{eff}, of BSCO, BPSCO, and NCO, which are transformed from the data in Fig. 2(b). The inset shows the effective carrier number in the low-energy regime.

Table 1

Table 1 Hall coefficients, R_H, and sheet carrier densities, *nd*, of NCO (x = 0.75), CCO, BSCO, and BPSCO. Data of R_H and *d* is taken from the previous reports [13-14, 34-37].

	NCO (x = 0.76)	CCO	BSCO	BPSCO
R_H (10^{-3}cm^3/C)	2.5	13	12	11
nd (10^{13}cm^{-2})	13	5.2	7.7	7.2

Figure 3

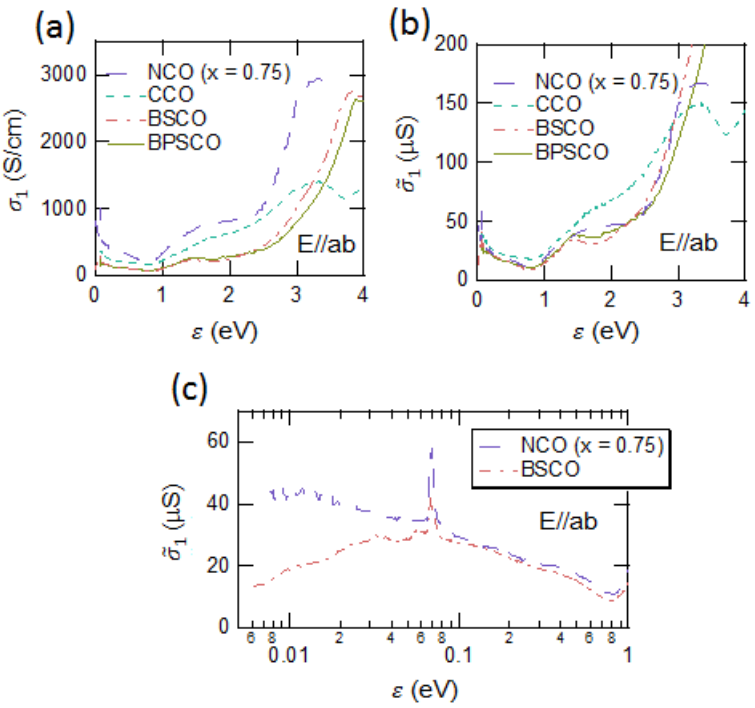

Fig. 3 (Color Online) (a) Optical conductivities, σ_1, of NCO (x = 0.75), CCO, BSCO, and BPSCO. (b) Optical sheet conductivities, $\tilde{\sigma}_1$, of NCO (x = 0.75), CCO, BSCO, and BPSCO. Data of NCO (x = 0.75) and CCO is taken from the previous reports [18,30]. (c) Extended optical sheet conductivities, $\tilde{\sigma}_1$, of NCO (x = 0.75) and BSCO in the low-energy regime below 1 eV.

Figure 4

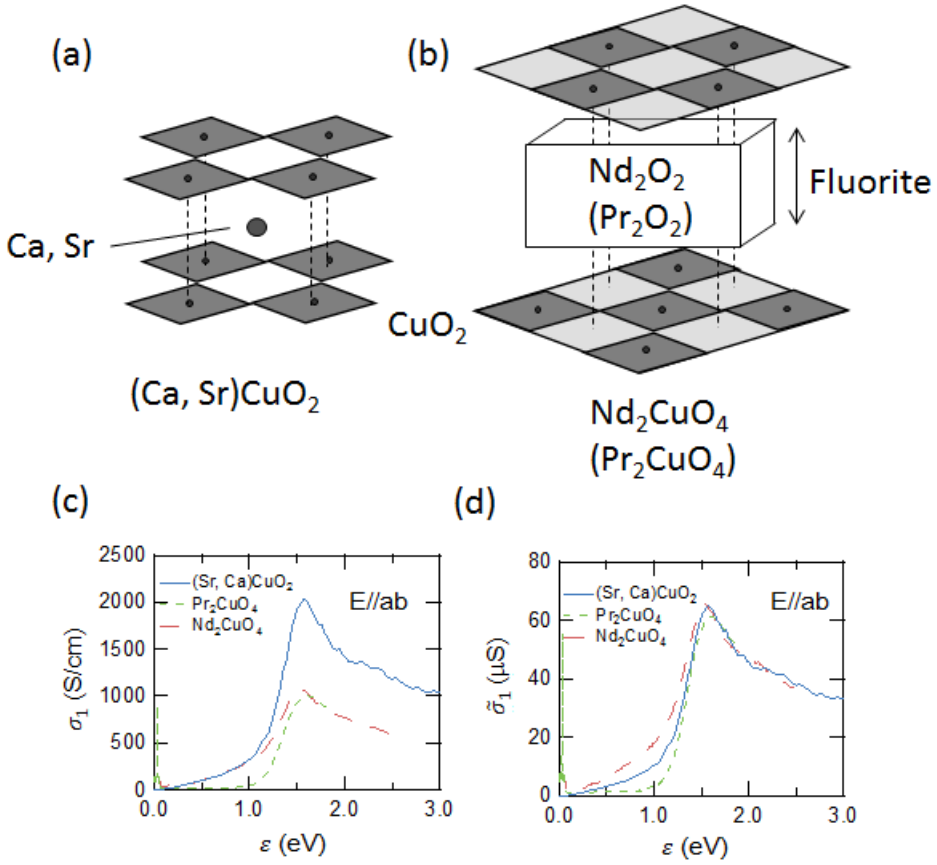

Fig. 4 (Color Online) (a) Crystal structure of (Ca, Sr)CuO_2. (b) Crystal structure of Nd_2CuO_4 (Pr_2CuO_4). (c) Optical conductivities, σ_1, of (Ca, Sr)CuO_2, Nd_2CuO_4 , and Pr_2CuO_4, which are taken from the previous reports [39–41]. (d) Optical sheet conductivities, $\tilde{\sigma}_1$, of (Ca, Sr)CuO_2, Nd_2CuO_4 , and Pr_2CuO_4, which are converted from data in Fig. 4(c).